



Angle-resolved photoemission spectroscopy of gallium arsenide using synchrotron radiation  
by James Arthur Knapp

A thesis submitted in partial fulfillment of the requirements for the degree of DOCTOR OF  
PHILOSOPHY in Physics  
Montana State University  
© Copyright by James Arthur Knapp (1976)

Abstract:

Angle-resolved photoemission spectroscopy is a relatively new, powerful technique for studying the electronic properties of solids. Measuring the direction as well as the energy of photoemitted electrons provides both energy and wavevector information about the electronic states of the material. To achieve this capability, a cylindrical mirror electron energy analyzer was modified to permit collection of photoemission spectra with  $4^\circ$  angular resolution. Since the parallel component of the electron's momentum (Formula not captured by OCR) is conserved upon leaving the sample, surface band structure information was directly accessible. Observed bulk transitions were limited by the technique to those which occur only along certain lines in (Formula not captured by OCR)-space. Three methods of photoemission spectroscopy were employed; angle-resolved electron energy distribution curves (EDO's), angle-resolved constant final energy spectra (CFS's), and angle-resolved constant initial energy spectra (CIS's).

Angle-resolved photoemission from the (110) face of Gallium Arsenide was studied using synchrotron radiation. The  $4^\circ$  resolution, in conjunction with the wide photon energy continuum of synchrotron radiation ( $h\nu < 30$  eV), permitted the gathering of considerable dispersion information about the electronic states of the material, both at the surface and in the bulk. Two occupied surface states were identified and portions of their band structure mapped out. The observed states, centered at  $\sim -1$  eV and  $\sim -6$  eV measured from the valence band maximum, have been predicted in several theoretical calculations, but have not been observed previously in experiment due to their degeneracy with bulk valence bands. Observations of bulk transitions concentrated on emission normal to the surface, for which the transitions occur primarily along the  $\zeta$  symmetry line in the bulk Brillouin zone. Data was collected for several different orientations of the electric polarization vector  $\epsilon$  relative to the crystal symmetries. A simple, direct-transition model proved sufficient to explain much of the phenomena, including the identification of several bulk energy band critical points.

ANGLE-RESOLVED PHOTOEMISSION SPECTROSCOPY OF GALLIUM ARSENIDE  
USING SYNCHROTRON RADIATION

by

JAMES ARTHUR KNAPP

A thesis submitted in partial fulfillment  
of the requirements for the degree

of

DOCTOR OF PHILOSOPHY

in

Physics

Approved:

  
Chairperson, Graduate Committee

  
Head, Major Department

  
Graduate Dean

MONTANA STATE UNIVERSITY  
Bozeman, Montana

November, 1976

## ACKNOWLEDGMENTS

The author is grateful for the support of the U. S. Air Force Office of Scientific Research, Air Force Systems Command, under Grants No. AFOSR 71-2061 and 75-2872. The guidance and encouragement of my thesis advisor, Gerald J. Lapeyre, is gratefully acknowledged. I am indebted to John Hermanson and Bill Schwalm for patient explanations of solid state theory. Thanks also to Jim Anderson, Dick Smith, and Pete Gobby for help with the experiment and for many fruitful discussions. I have benefited greatly from the work of electronic technicians Fred Blankenburg and Jay Walker, machinist Cecil Badgley, and Physics Laboratory Supervisor Mark Baldwin. I am indebted to Neville Smith, Morton Traum, and Jack Rowe of Bell Laboratories for their assistance in the early part of the work, as well as several valuable discussions. A special thanks to Kosal Pandey for supplying the calculated energy bands of GaAs. I am especially indebted to Ednor Rowe, Roger Otte, and the rest of the staff of the University of Wisconsin Synchrotron Radiation Center for their cheerful help and encouragement over many long weeks of data collection.

Finally, my loving thanks to my wife Alice for her love and encouragement over the years, shown most recently in the typing of this manuscript.

## TABLE OF CONTENTS

	Page
VITA . . . . .	iii
ACKNOWLEDGMENT . . . . .	iv
LIST OF TABLES . . . . .	viii
LIST OF FIGURES . . . . .	ix
ABSTRACT . . . . .	xiii
I. INTRODUCTION . . . . .	1
II. THE PHYSICS OF PHOTOEMISSION SPECTROSCOPY . . . . .	7
A. Energy Bands of Solids . . . . .	7
1. Band Theory . . . . .	7
2. Repeated Zone Scheme . . . . .	10
B. The Three Modes of Photoemission Spectroscopy . . . . .	11
1. Photoemission . . . . .	11
2. Electron Energy Distribution Curve . . . . .	14
3. Constant Final Energy Spectra . . . . .	16
4. Constant Initial Energy Spectra . . . . .	18
C. Angle-Resolved Photoemission Spectroscopy . . . . .	20
1. Direct vs. Indirect Transitions . . . . .	21
2. Transport and Escape . . . . .	24
3. Measurement of Surface State Bands . . . . .	26
4. Identification of Bulk Transitions . . . . .	27
D. The Structure of GaAs . . . . .	28
1. Bulk Lattice and Brillouin Zone . . . . .	28
2. (110) Surface and Surface Brillouin Zone . . . . .	29
III. EXPERIMENTAL EQUIPMENT AND PROCEDURES . . . . .	35
A. Synchrotron Radiation Source . . . . .	35

	Page
B. Experimental Chamber . . . . .	39
C. Angle-Resolving Analyzer . . . . .	41
D. Analyzer/Sample Orientation . . . . .	49
1. Emission Cone Orientations . . . . .	49
2. Polarization Mounting . . . . .	53
E. Analyzer Electronics . . . . .	57
F. Sample Preparation . . . . .	60
1. Source of GaAs Crystals . . . . .	60
2. Mounting and Cleaving . . . . .	60
3. Symmetry Determination . . . . .	63
IV. EXPERIMENTAL RESULTS . . . . .	65
A. GaAs Bands and Photoemission . . . . .	65
1. Calculated Band Structure . . . . .	65
2. Angle-Resolved Photoemission and Symmetry . . . . .	69
3. Initial vs. Final Energy Dependence . . . . .	72
4. Polarization Effects . . . . .	76
B. Occupied Surface States . . . . .	81
1. Surface Calculations and UPS Measurements . . . . .	81
2. Tests of Surface State Emission . . . . .	84
3. Surface State $B_1$ . . . . .	85
4. Surface State $B_2$ . . . . .	97
C. Unoccupied Surface State . . . . .	101
1. Calculations and Experimental Measurements . . . . .	101
2. Angle-Resolved Observations . . . . .	103
3. Surface Contamination Sensitivity . . . . .	105
D. Bulk Band Structure Determination . . . . .	108
1. Normal Emission . . . . .	108

	Page
2. Initial Band Critical Points . . . . .	114
3. Final Band Structure . . . . .	120
4. Polarization Dependence . . . . .	133
V. SUMMARY . . . . .	140
APPENDIX . . . . .	145
REFERENCES . . . . .	153

LIST OF TABLES

Table	Page
I. Energies of selected initial band critical points in GaAs relative to the VBM . . . . .	119
II. Energies of selected final band critical points in GaAs relative to the VBM . . . . .	132

## LIST OF FIGURES

Figure	Page
1. Energy band structure along the (110) direction in k-space for three different crystal potentials . . . . .	9
2. Schematic of the Electron Energy Distribution Curve mode of photoemission spectroscopy . . . . .	15
3. Schematic of the Constant Final Energy Spectrum . . . . .	17
4. Schematic of the Constant Initial Energy Spectrum . . . . .	19
5. Schematic of two types of transitions . . . . .	22
6. Relationship between components of the electron wavevector before and after emission from the solid . . . . .	25
7. GaAs space lattice . . . . .	30
8. GaAs bulk Brillouin zone . . . . .	31
9. (110) surface lattice . . . . .	33
10. (110) surface Brillouin zone . . . . .	34
11. Tantalus I storage ring . . . . .	36
12. Light curve . . . . .	38
13. Schematic of the experimental chamber . . . . .	40
14. CMA in angle-integrating mode . . . . .	43
15. CMA in angle-resolving mode . . . . .	45
16. Angle-resolving CMA modification . . . . .	46
17. Sample/emission cone orientation for sample normal aligned with CMA axis . . . . .	50

Figure	Page
18. Sample/emission cone orientation for sample normal 42.3° from the CMA axis . . . . .	52
19. "Polarization" sample manipulator . . . . .	54
20. Photograph of polarization sample manipulator . . . . .	56
21. Analyzer and associated electronics . . . . .	58
22. Photograph of the sample holder and a GaAs chip . . . . .	62
23. Bulk band structure of GaAs . . . . .	66
24. Angle-integrated EDC obtained at $h\nu = 30$ eV . . . . .	68
25. Angle-resolved EDC's obtained at $h\nu = 14$ eV . . . . .	70
26. (110) GaAs $\phi$ -pattern . . . . .	73
27. (110) GaAs $\phi$ -patterns . . . . .	75
28. AREDC's obtained for two different polarization orientations . . . . .	78
29. AREDC's showing surface state emission which is reduced by contamination . . . . .	87
30. AREDC's taken at constant $\phi = 180^\circ$ and $\theta = 70^\circ$ . . . . .	89
31. Initial energy $E_i$ versus $\vec{k}_{  }$ for the surface emission peaks from AREDC's . . . . .	90
32. $\phi$ -pattern for $\vec{k}_{  } = 1.11 \text{ \AA}^{-1}$ . . . . .	92
33. $\phi$ -pattern for $\vec{k}_{  } = 1.54 \text{ \AA}^{-1}$ . . . . .	94
34. A cross-section of the repeated bulk Brillouin zones for GaAs . . . . .	96
35. AREDC's showing the effect of contamination on emission attributed to the surface state $B_2$ . . . . .	98

Figure	Page
36. AREDC's taken at constant $h\nu = 18$ eV and $\theta = 60^\circ$ . . . . .	100
37. Normal emission ARCIS's exhibiting surface exciton resonance emission . . . . .	104
38. Normal emission AREDC's obtained at either side of and on the surface exciton resonance . . . . .	106
39. Contamination test CFS's for exciton resonance emission and surface state $B_1$ . . . . .	107
40. Normal emission AREDC's obtained with $\vec{\epsilon}$ at $\theta_A = 47.7^\circ$ and $\phi_A = 0^\circ$ . . . . .	111
41. Normal emission ARCFS's obtained with $\vec{\epsilon}$ at $\theta_A = 47.7^\circ$ and $\phi_A = 0^\circ$ . . . . .	112
42. Normal emission ARCIS's obtained with $\vec{\epsilon}$ at $\theta_A = 47.7^\circ$ and $\phi_A = 0^\circ$ . . . . .	113
43. ARCFS obtained at normal emission . . . . .	116
44. ARCFS exhibiting emission from valence bands along $L \rightarrow W$ . . . . .	118
45. ARCIS showing transitions from near $\Gamma_{15}$ along $\Sigma$ . . . . .	122
46. ARCIS showing transitions from initial bands at $E_i = -1.8$ eV . . . . .	125
47. ARCIS showing transitions from initial bands at $E_i = -2.8$ eV . . . . .	127
48. ARCIS showing transitions from initial bands at $E_i = -4.05$ eV . . . . .	129
49. ARCIS showing transitions from initial bands at $E_i = -6.55$ eV . . . . .	131
50. AREDC's exhibiting s polarization dependence . . . . .	134
51. AREDC's exhibiting p polarization dependence . . . . .	138

Figure	Page
52. Normal emission AREDC's obtained with $\vec{\epsilon}$ at $\theta_A = 47.7^\circ$ and $\phi_A = 180^\circ$ . . . . .	147
53. Normal emission ARCIS's obtained with $\vec{\epsilon}$ at $\theta_A = 47.7^\circ$ and $\phi_A = 180^\circ$ . . . . .	148
54. Normal emission AREDC's obtained with $\vec{\epsilon}$ at $\phi_A = 0^\circ$ in s polarization . . . . .	149
55. Normal emission ARCIS's obtained with $\vec{\epsilon}$ at $\phi_A = 0^\circ$ in s polarization . . . . .	150
56. Normal emission AREDC's obtained with $\vec{\epsilon}$ at $\phi_A = 90^\circ$ in s polarization . . . . .	151
57. Normal emission ARCIS's obtained with $\vec{\epsilon}$ at $\phi_A = 90^\circ$ in s polarization . . . . .	152

## ABSTRACT

Angle-resolved photoemission spectroscopy is a relatively new, powerful technique for studying the electronic properties of solids. Measuring the direction as well as the energy of photoemitted electrons provides both energy and wavevector information about the electronic states of the material. To achieve this capability, a cylindrical mirror electron energy analyzer was modified to permit collection of photoemission spectra with  $4^\circ$  angular resolution. Since the parallel component of the electron's momentum  $\hbar\vec{k}_{\parallel}$  is conserved upon leaving the sample, surface band structure information was directly accessible. Observed bulk transitions were limited by the technique to those which occur only along certain lines in  $\vec{k}$ -space. Three methods of photoemission spectroscopy were employed; angle-resolved electron energy distribution curves (EDC's), angle-resolved constant final energy spectra (CFS's), and angle-resolved constant initial energy spectra (CIS's).

Angle-resolved photoemission from the (110) face of Gallium Arsenide was studied using synchrotron radiation. The  $4^\circ$  resolution, in conjunction with the wide photon energy continuum of synchrotron radiation ( $h\nu < 30$  eV), permitted the gathering of considerable dispersion information about the electronic states of the material, both at the surface and in the bulk. Two occupied surface states were identified and portions of their band structure mapped out. The observed states, centered at  $\sim -1$  eV and  $\sim -6$  eV measured from the valence band maximum, have been predicted in several theoretical calculations, but have not been observed previously in experiment due to their degeneracy with bulk valence bands. Observations of bulk transitions concentrated on emission normal to the surface, for which the transitions occur primarily along the  $\Sigma$  symmetry line in the bulk Brillouin zone. Data was collected for several different orientations of the electric polarization vector  $\vec{\epsilon}$  relative to the crystal symmetries. A simple, direct-transition model proved sufficient to explain much of the phenomena, including the identification of several bulk energy band critical points.

## I. INTRODUCTION

Most of the observed properties of solids are determined by the electronic structure of the valence, or outer shell electrons. Elucidation of this structure is therefore a primary concern of those interested in understanding and predicting the behavior of solid materials under various conditions. There have been many theoretical and experimental efforts applied to this end over the years.<sup>1</sup> The development of large-capacity, high-speed computers has facilitated the development of several approaches to calculating the electronic structure (band structure) of metals, insulators, and semiconductors. These techniques are all based on the one-electron approximation, which has proved its value in comparison to experiment. Experimental methods for determining the energy and wavefunctions of the electrons in solids have centered on exciting those electrons to higher energy states with either photons or other electrons. Information about the transitions is then derived from measurements of the rate of excitation, such as an optical absorption spectrum, or from measurements of electrons which are ejected from the material after excitation. Conventional angle-integrated ultraviolet photoemission spectroscopy (UPS) is of the latter type of measurement. Electrons which are excited to sufficient energy by the incident ultraviolet light may be

emitted from the solid and detected. The number of these photoelectrons as a function of kinetic energy provides much useful information about the strength and energies of the optical transitions. However, since the detection includes all or most of the emission hemisphere, any information which may be contained in the directional dependence of the emission is lost. None of the conventional experimental techniques, including UPS, provide much information about the wavevectors of the electron wavefunctions, in general measuring all transitions regardless of origin in reciprocal lattice space.

In 1964, Gobel, Allen, and Kane<sup>2</sup> demonstrated that a substantial portion of photoemitted electrons escape the sample without losing momentum to phonons or imperfections in the bulk or at the surface. For these electrons, the component of wavevector parallel to the surface is conserved, while the perpendicular component is modified in the process of escape. This demonstration of wavevector conservation implied that, subject to certain limitations, both the energy and the wavevector of the valence electrons might be measured by determining the energy and direction of photoemitted electrons. Mahan calculated in 1970 that the photoemission from a free-electron-like metal (sodium) should have a highly anisotropic angular distribution.<sup>3</sup> Tentative experimental work proceeded at several laboratories, concentrating on the variation of emission

with polar angle<sup>4-7</sup> or on emission from several crystal faces.<sup>8</sup> The first study of both polar and azimuthal dependence of photoemission was done, coincidentally enough, on the (110) face of GaAs at a photon energy of 10.2 eV by Smith and Traum in 1973.<sup>9</sup> Interpretation of these spectra was inhibited by the lack of conservation of the perpendicular component of momentum.<sup>9,10</sup> Further experiments by Smith and his co-workers on two-dimensional systems, such as the layered compound TaS<sub>2</sub><sup>11,12</sup> and surface states on Si(111),<sup>13,14</sup> provided for the first time tangible success in actually mapping out energy bands with experiment. Angle-resolved photoemission spectroscopy was beginning to show substantial promise.

Concurrently with the early development of angle-resolved photoemission spectroscopy, the use of synchrotrons and storage rings as a source of radiation began to receive ever increasing attention.<sup>15</sup> In accelerators or storage rings, electrons radiate as they are accelerated by bending magnets. In their frame of reference, the electrons radiate in a Larmor radiation pattern, but in the laboratory frame, with a velocity approaching that of light, they radiate strongly in the forward direction. This synchrotron radiation, as it is called, is a highly collimated, intense, continuous spectrum, which includes many photon energies not available from other sources. The use of a monochromator with the radiation provides a continuously tunable source that in the last

ten years has been used in a wide variety of experimental applications. Facilities to provide this radiation to research groups have been built around the world, including three in the U.S. One is the synchrotron radiation facility at SPEAR, the electron-positron ring in California. Another is SURF-II, a storage ring at the National Bureau of Standards in Washington, D.C. The third is Tantalus I, a 240 MeV storage ring at the University of Wisconsin, which provides synchrotron radiation for groups from around the country. Tantalus I was the first facility dedicated completely to providing synchrotron radiation for research. The Montana State University photoemission group has been using the Wisconsin facility since 1971 for photoemission studies.

The use of synchrotron radiation as an excitation source for doing angle-resolved photoemission spectroscopy is a natural development that greatly enhances an already promising technique. The wide continuum of photon energy permits the study of a large region of momentum and energy space. Furthermore, the radiation is strongly polarized in the plane of the electron's orbit, adding still another factor in the optical transition which can be investigated.

A primary purpose of this research project has been to develop equipment and techniques, compatible with existing equipment, with which angle-resolved photoemission spectroscopy could be performed

on single crystals using synchrotron radiation. This goal was attained. Preliminary studies of  $TaS_2$ , done in collaboration with N.V. Smith and M.M. Traum of Bell Laboratories using the equipment to be described herein, are believed to be the first studies of this kind on single crystals using synchrotron radiation.<sup>16,17</sup>

Another goal of the research project has been to demonstrate the usefulness of the technique by a careful study of a material which is interesting from both theoretical and application standpoints. GaAs was chosen as the subject of the study for several reasons. First, clean (110) surfaces could be prepared in situ by cleaving, simplifying sample preparation. Second, several theoretical calculations of bands exist with which the data could be compared, both in the bulk<sup>18-20</sup> and at the surface.<sup>21-25</sup> Lastly, GaAs is an important semiconductor in terms of its present and potential application to solid-state devices.

The study was successful in identifying surface states at  $\sim 1$  eV and  $\sim 6$  eV below the Fermi level. These states had been predicted by the theoretical calculations,<sup>22-25</sup> but not previously observed in experiment.<sup>26</sup> Bulk energy band positions were identified that are difficult to discern in conventional photoemission. Emission from initial states located at  $\Sigma_1^{\min}$ ,  $X_5$ , and  $L_3$  was isolated, fixing the energy position of these levels more positively than has been previously possible. Several conduction band energy

levels were identified, many of which have been inaccessible with other techniques. The bulk emission features, as a whole, correlated very well with existing band calculations, providing confidence in the one-electron approximation and demonstrating a valuable technique for checking and refining future band calculations.

The discussion of the project will begin with a short review of the band theory of solids and the optical transition which is the source of photoemitted electrons. The three modes of collecting photoemission spectra are presented, with particular emphasis given to methods of data analysis unique to angle-resolved photoemission spectroscopy. The experimental details are then discussed in Chapter III, including a description of the angle-resolving modification of the electron energy analyzer. Sample preparation and orientation is detailed. Chapter IV compiles the experimental results. Emission from the two occupied surface states is described, along with tests of its surface character. Observations of an unoccupied surface state are presented and compared to results from other experiments. Finally, emission due to bulk transitions is detailed, with demonstrations of bulk band critical point identifications. The last chapter summarizes the experiment and its results.

## II. THE PHYSICS OF PHOTOEMISSION SPECTROSCOPY

### A. Energy Bands of Solids

1. Band Theory. The one-electron approximation is the basis of the band theory of solids.<sup>1</sup> The electron is assumed to behave as an isolated entity immersed in a potential due to the periodic array of atomic cores plus an overall potential due to the other valence electrons. All wave functions are then single-electron wave functions. The solutions of the Schrodinger equation

$$\left\{ \left( \frac{1}{2m} \right) \vec{p}^2 + V(\vec{r}) \right\} \psi = E\psi \quad (1)$$

for a periodic crystal potential  $V(\vec{r})$  are Bloch functions

$$\psi(\vec{k}, \vec{r}) = U_{\vec{k}}(\vec{r}) e^{i\vec{k} \cdot \vec{r}} \quad (2)$$

where  $U_{\vec{k}}(\vec{r})$  is a function with the periodicity of the lattice.

The simplest solution to Eq. (1) is for the case  $V(\vec{r}) = 0$ , the "free electron" solution. The wave functions are then plane waves and the energy of an electron is given by

$$E = \hbar^2 k^2 / 2m \quad (3)$$

The energy vs. wavevector relation in Eq. (3) embodies the electron energy bands for the free electron. Energy here is a simple parabolic function of  $\vec{k}$ . If we include the lattice periodicity, leaving

the potential arbitrarily weak, we can write

$$E = \left( \frac{\hbar^2}{2m} \right) |\vec{k} + \vec{G}|^2 \quad (4)$$

where  $\vec{G}$  is a reciprocal lattice vector. The bands can then be represented in the reduced zone scheme. Figure 1a shows the free electron bands plotted along the (110) direction in the reduced zone. As the potential  $V(\vec{r})$  is "turned on" partially, degeneracies are lifted and band crossings eliminated, resulting in the "nearly free" electron energy bands of Fig. 1b. The energy bands for the complete potential for GaAs<sup>20</sup> are shown in Fig. 1c, with the bands labelled according to the symmetry points and the Fermi energy  $E_F$  indicated. The crystal field has produced an energy gap of 1.4 eV between the bands below the Fermi energy and those above. Those states represented by the bands below  $E_F$  are normally occupied at room temperature and are called the valence bands (VB's) while the states which lie above  $E_F$  are unoccupied and called conduction bands (CB's). The location of  $E_F$  in the band gap is of course determined by the impurity doping of the material, but this study concentrated on p-type GaAs, putting  $E_F$  at the bottom of the gap. The spin-orbit interaction, when included, will split even more degeneracies, but this effect is smaller than our experimental resolution<sup>19</sup> and will be neglected in the interpretation of the results.

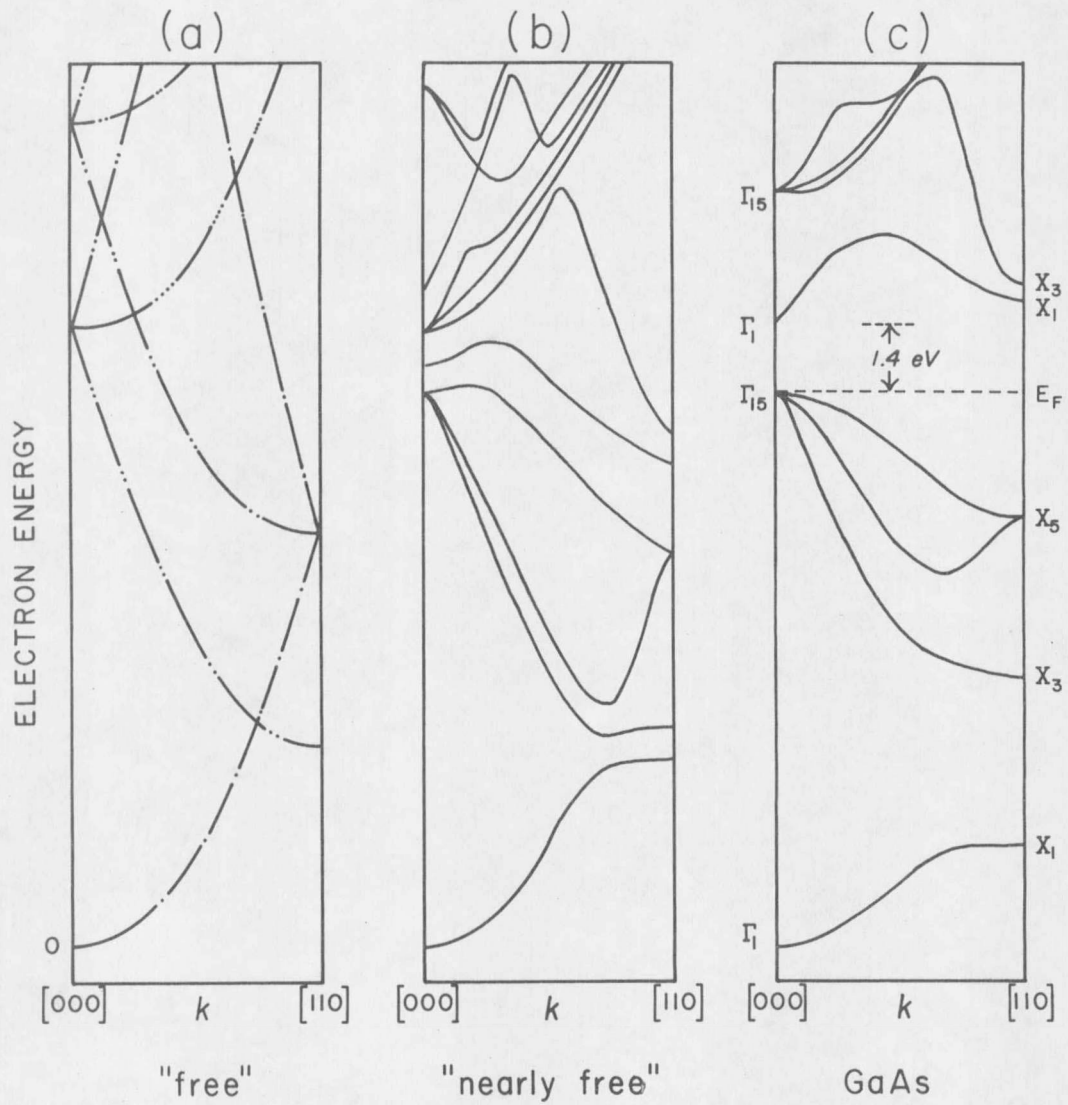


FIG. 1. Energy band structure along the  $(110)$  direction in  $k$ -space for three different crystal potentials.

2. Repeated Zone Scheme. The concept of a repeated zone scheme should be expanded upon, since its use is central to the data interpretation. If we encounter a Bloch wavefunction written as in Eq. (2) with  $\vec{k}$  lying outside the first zone, we can always find a reciprocal lattice vector  $\vec{G}$  such that

$$\vec{k}' = \vec{k} - \vec{G} \quad (5)$$

lies inside the first zone. We then rewrite Eq. (2) as

$$\begin{aligned} \Psi(\vec{k}', \vec{r}) &= U_{\vec{k}'}(\vec{r}) e^{i\vec{k}' \cdot \vec{r}} = (e^{i\vec{G} \cdot \vec{r}} U_{\vec{k}'}(\vec{r})) e^{i\vec{k} \cdot \vec{r}} \\ &= U_{\vec{k}}(\vec{r}) e^{i\vec{k} \cdot \vec{r}} \\ &= \Psi(\vec{k}, \vec{r}) \end{aligned} \quad (6)$$

where

$$U_{\vec{k}}(\vec{r}) = (e^{i\vec{G} \cdot \vec{r}} U_{\vec{k}'}(\vec{r})) \quad (7)$$

is periodic in the lattice as required. It follows that energy  $E_{\vec{k}}$  outside the first zone is equal to an  $E_{\vec{k}'}$  inside the first zone. Translating the bands back into the first zone is the basis of the reduced zone scheme. Since the bands can be translated back into the first zone with appropriate reciprocal lattice vectors, they can also be translated to any other or every zone. Then the bands become periodic in the reciprocal lattice:

$$E_{\mathbf{k}} = E_{\mathbf{k}+\mathbf{G}} \quad (8)$$

This procedure is called the repeated, or periodic zone scheme. It is of use in the interpretation of the data because the results may be plotted in reciprocal lattice space directly, without adding or subtracting reciprocal lattice vectors to translate everything back to the first zone. The repeated zone scheme may be thought of as an unfolding of a wavevector description (reduced zone scheme) into a "momentum space". In this "momentum space", each band has a different "momentum" weighting in each repeated zone. The word "momentum" is used somewhat loosely here, since a wavevector  $\vec{k}$  is directly proportional to momentum only for a free particle.

## B. The Three Modes of Photoemission Spectroscopy

1. Photoemission. When light of sufficient energy shines on a material, it may excite a transition between a filled valence state and an empty conduction state. If the final state has sufficient energy, the electron may escape the solid as a photoemitted electron, either with or without undergoing a scattering event. The Hamiltonian  $H$  including the electron-photon interaction, with the charge of the electron as  $-e$ , is

$$H = \frac{1}{2m} \left( \vec{p} + \frac{e}{c} \vec{A} \right)^2 + V(\vec{r}) \quad (9)$$

where  $\vec{A}$  is the vector potential of the radiation field.<sup>27</sup> Letting  $\vec{\nabla} \cdot \vec{A} = 0$  and dropping terms of order  $A^2$ , Eq. (9) reduces to

$$H = \frac{1}{2m} \vec{p}^2 + V(\vec{r}) + \frac{e}{mc} \vec{A} \cdot \vec{p} \quad (10)$$

The first two terms are just the unperturbed Hamiltonian  $H_0$ . The last we shall call the perturbing Hamiltonian  $H_{if}$ .

$$H_0 = \frac{1}{2m} \vec{p}^2 + V(\vec{r}), \quad H_{if} = \frac{e}{mc} \vec{A} \cdot \vec{p} \quad (11)$$

Using Fermi's Golden Rule of time-dependent perturbation theory,<sup>27</sup> the transition rate  $W_{if}$  for excitation from an initial density of states  $N_i$  at initial energy  $E_i = E - h\nu$  to a final density of states  $N_f$  at final energy  $E_f = E$  is

$$W_{if} = \frac{2\pi}{\hbar} \{ \langle f | \left( \frac{e}{mc} \vec{A} \cdot \vec{p} \right) | i \rangle \}^2 N_i(E - h\nu) N_f(E) \quad (12)$$

Energy conservation has been put into the formula explicitly, using  $E_i = E_f - h\nu$ . The initial and final state wave functions are indicated as  $|i\rangle$  and  $\langle f|$  respectively. The quantity which is squared in Eq. (12) is called the matrix element and is in general not known, since we lack exact forms for the wave functions.

Substitution of Bloch wave functions into a more general form of Eq. (12) also leads to a selection rule between initial and final

wavevectors.<sup>28</sup> Without interaction with lattice imperfections or phonons, the transition is allowed only between wavefunctions with the same reduced wavevector. Transitions fulfilling this requirement are termed direct transitions and will be discussed in more detail later.

Neglecting for the moment the directionality of the emission, the number of electrons emitted with a particular final energy  $E$  is then basically proportional to the initial density of states (DOS) which are excited to that energy convoluted with the final DOS at that energy. This simple convolution is modulated by the matrix elements and added to or subtracted from by inelastic scattering. The emission intensity at all possible combinations of initial and final DOS at all  $h\nu$  constitutes a three-dimensional surface which we shall call the emission surface. The axes of this surface are photoemission intensity  $N(E_i, E_f, h\nu)$ , photon energy  $h\nu$ , and final energy  $E_f$ . (Again, this discussion neglects the directionality of the emission; such an emission surface exists for each direction of emission and also for the total, angle-integrated emission.) In studying the photoemission from solids, we have used three different modes of photoemission spectroscopy to analyze the emission surface in three different but complementary ways. These three modes are Electron Energy Distribution Curves, Constant Final Energy Spectra, and Constant Initial Energy Spectra.

2. Electron Energy Distribution Curves. The first method of photoemission spectroscopy is also the most established, the Electron Energy Distribution Curve (EDC). In this mode the photon energy  $h\nu$  is fixed and the intensity of emission as a function of kinetic energy in the vacuum is recorded. Figure 2 shows a schematic of this process. Valence and conduction band DOS are shown as cross-hatched areas on the left side, representing the sample. The right side represents the vacuum, with the vacuum level  $E_v$  indicated. (The vertical axis in the figure is energy.)  $E_v$  is the minimum final energy for which an electron may escape the solid. The fundamental threshold for emission of an electron into the vacuum is  $E_{th}$ , the difference between  $E_v$  and the top of the valence bands at  $E_{vbm}$ . The work function  $\Phi$  is the difference between  $E_v$  and  $E_F$ . For heavily doped p-type semiconductors,  $\Phi$  corresponds to  $E_{th}$ . The measured kinetic energy  $E_k$  of an unscattered photoelectron is

$$E_k = h\nu + E_i - E_{th} \quad (13)$$

where  $E_i$  is measured relative to the top of the valence bands at  $E_F$ . Since  $h\nu$  and  $E_{th}$  are fixed, Eq. (13) shows that the EDC measures a spectrum of initial energies, each excited to a different final energy.

Two types of photoelectrons are shown in Fig. 2, a "primary"































































































































































































































































































